ANNALS OF BOTANY
Founded 1887

PART OF A SPECIAL ISSUE ON POLYPLOIDY IN ECOLOGY AND EVOLUTION

Hybridization and introgression are prevalent in Southern European *Erysimum* (Brassicaceae) species

Carolina Osuna-Mascaró[1,2,3,*], **Rafael Rubio de Casas**[2,4], **José M. Gómez**[2,5], **João Loureiro**[6], **Silvia Castro**[6,],
Jacob B. Landis[7,8], **Robin Hopkins**[9,10] and **Francisco Perfectti**[1,2,*]

[1]Departamento de Genética, Universidad de Granada, Granada, Spain, [2]Research Unit Modeling Nature, Universidad de Granada, Granada, Spain, [3]Department of Biology, University of Nevada, Reno, 1664 North Virginia Street, Reno, NV 89557-0314, USA, [4]Departamento de Ecología, Universidad de Granada, Granada, Spain, [5]Departamento de Ecología Funcional y Evolutiva, Estación Experimental de Zonas Áridas (EEZA-CSIC), Almería, Spain, [6]Centre for Functional Ecology, Department of Life Sciences, University of Coimbra, Coimbra, Portugal, [7]BTI Computational Biology Center, Boyce Thompson Institute, Ithaca, NY 14853, USA, [8]School of Integrative Plant Science, Section of Plant Biology and the L.H. Bailey Hortorium, Cornell University, Ithaca, NY, USA, [9]Department of Organismic and Evolutionary Biology, Harvard University, Cambridge, MA, USA and [10]The Arnold Arboretum, 1300 Centre Street, Boston, MA, USA
*For correspondence. E-mail cosuna@unr.edu or fperfect@ugr.es

• **Background and Aims** Hybridization is a common and important force in plant evolution. One of its outcomes is introgression – the transfer of small genomic regions from one taxon to another by hybridization and repeated backcrossing. This process is believed to be common in glacial refugia, where range expansions and contractions can lead to cycles of sympatry and isolation, creating conditions for extensive hybridization and introgression. Polyploidization is another genome-wide process with a major influence on plant evolution. Both hybridization and polyploidization can have complex effects on plant evolution. However, these effects are often difficult to understand in recently evolved species complexes.
• **Methods** We combined flow cytometry, analyses of transcriptomic sequences and pollen tube growth assays to investigate the consequences of polyploidization, hybridization and introgression on the recent evolution of several *Erysimum* (Brassicaceae) species from the South of the Iberian Peninsula, a well-known glacial refugium. This species complex differentiated in the last 2 million years, and its evolution has been hypothesized to be determined mainly by polyploidization, interspecific hybridization and introgression.
• **Key Results:** Our results support a scenario of widespread hybridization involving both extant and 'ghost' taxa. Several taxa studied here, most notably those with purple corollas, are polyploids, probably of allopolyploid origin. Moreover, hybridization in this group might be an ongoing phenomenon, as pre-zygotic barriers appeared weak in many cases.
• **Conclusions** The evolution of *Erysimum* spp. has been determined by hybridization to a large extent. Species with purple (polyploids) and yellow flowers (mostly diploid) exhibit a strong signature of introgression in their genomes, indicating that hybridization occurred regardless of colour and across ploidy levels. Although the adaptive value of such genomic exchanges remains unclear, our results demonstrate the significance of hybridization for plant diversification, which should be taken into account when studying plant evolution.

Key words: Hybridization, introgression, polyploidy, allopolyploidy, glacial refugium, Brassicaceae, *Erysimum* spp.

INTRODUCTION

Hybridization is widespread across the tree of life, determining the branching and diversification patterns of many taxonomic groups (Rieseberg and Carney, 1998; Coyne and Orr, 2004; Abbott *et al.*, 2013; Arnold, 2015). Because of its pervasiveness, hybridization has been a subject of research for a long time (Stebbins, 1959; Anderson, 1953; Arnold *et al.*, 1999). However, it is only recently, with the advent of next-generation sequencing, that scientists have started to analyse the dynamics of hybridization at the scale of whole genomes, thus rekindling interest in the evolutionary relevance of this phenomenon. Although the patterns of hybridization remain unexplored for many groups, the renewed research efforts have undoubtedly increased our understanding of the role of hybridization in nature (Payseur and Rieseberg, 2016; Goulet *et al.*, 2017; Taylor and Larson, 2019).

Hybridization is particularly relevant for plant evolution, with many plant species showing hybrid origins (Mallet, 2005; Soltis and Soltis, 2009). The evolutionary outcomes of hybridization may vary widely. Interspecific hybridization can hinder speciation and therefore diversification (Mayr, 1992; Schemske, 2000; Mallet, 2005; Saari and Faeth, 2012; Gómez *et al.* 2015a); however, in other cases, hybridization can actually foster the formation of new species (Rieseberg *et al.*, 2003; Stelkens and Seehausen, 2009) or

the introgression of novel genetic variation (by hybridization and repeated backcrossing; Anderson and Hubricht, 1938; Anderson, 1953; Rieseberg and Wendel, 1993). In addition, the fusion of genomes between two hybridizing species can lead to changes in ploidy levels (i.e. allopolyploidization; Soltis *et al.*, 2014). There is evidence that introgression might even span ploidy levels (e.g. gene flow between diploid and tetraploid species of *Senecio*; Chapman and Abbott, 2010), which led to intriguing questions about the interplay of introgression and polyploidization. However, the specifics of how hybridization, introgression and polyploidization interact to affect the evolution of particular plant groups remain poorly understood. Advancements in genomic sequencing technology and analyses are now making the challenges of characterizing these processes far more feasible, even in recently diverged lineages and taxa.

Erysimum L. is one of the largest genera of the Brassicaceae, comprising >200 species (Polatschek, 1986), and has been described as a taxonomically complex genus with a reticulated evolutionary history in which polyploidization may have affected the evolution of some clades (Marhold and Lihová, 2006; Turner, 2006; Abdelaziz, 2013; Muñoz-Pajares, 2013). This genus is distributed mainly in Eurasia, with some species in North America and North Africa (Warwick *et al.*, 2006). Notably, more than a hundred species have been described in the Mediterranean region (Greuter *et al.*, 1986), with particular abundance in the Iberian Peninsula, where 21 (Polatschek, 1978, 2014) or 23 (Nieto-Feliner, 1993; Mateo *et al.*, 1998) species have been described. Most Iberian *Erysimum* species have yellow flowers, but six have purple corollas (Nieto-Feliner, 1993; Gómez *et al.*, 2015b). Interestingly, previous studies suggested that some purple species may have a recent, hybrid and allopolyploid origin (Nieto-Feliner, 1992, 1993; Abdelaziz *et al.*, 2014; Gómez *et al.*, 2014). A history of hybridization could further suggest the possibility that the purple flower colour has been transferred across the Iberian clade through hybridization and then maintained by natural selection. This scenario would indicate that introgression and polyploidization are intertwined in this group and might have contributed to the adaptive evolution of *Erysimum* spp.

Here we studied signals of hybridization across six species of *Erysimum* (*E. mediohispanicum*, *E. nevadense*, *E. fitzii*, *E. popovii*, *E. baeticum* and *E. bastetanum*) that inhabit the Baetic Mountains, an important and dynamic glacial refugium (Médail and Diadema, 2009). The evolution of several plant species has been hypothesized to have been affected by speciation and secondary contacts in this region (Médail and Diadema, 2009; Nieto-Feliner, 2011). The repeated expansion and contraction of ranges and the subsequent cycles of sympatry and isolation might have created conditions for extensive hybridization, introgression and allopolyploid formation. This species group appears to have differentiated relatively rapidly within the last 2 million years (Osuna-Mascaró *et al.*, 2021). Previous authors have hypothesized that this rapid evolution has been strongly affected by polyploidization and hybridization, as this group spans several ploidy levels, and some species pairs have been reported to produce fertile hybrids (Abdelaziz *et al.*, 2014, 2021). Species of this group show characteristics that may facilitate ongoing introgression, such as growing in sympatry in some locations and having a generalist pollination system that enables gene flow among different species possible.

The main goal of this study is to disentangle the history of hybridization for the *Erysimum* species complex in the Baetic Mountains. Specifically, we considered both whole-genome effects of hybridization (i.e. the interplay between hybridization and polyploidization) and local, potentially important, introgression of specific genomic regions. Moreover, we also quantified pre-zygotic barriers among extant taxa to estimate the likelihood of gene flow among them. We test the hypotheses that (1) genomes of this species complex must exhibit signals of multiple hybridization events; (2) some taxa might be allopolyploid; and (3) if purple corollas are the product of introgression, hybridization and gene flow should be detectable, and pre-zygotic barriers may be weak between (at least some) yellow and purple taxa.

MATERIALS AND METHODS

Plant samples

We studied six species in the genus *Erysimum* collected in the Baetic Mountains, South of Spain (Table 1; Fig. 1). Specifically, we sampled three different populations for *E. mediohispanicum*

TABLE 1. *Population code, location and details of sympatry status for all of the populations sampled*

Species	Population	Location	Elevation	Geographical co-ordinates	Flower colour	Sympatry with
E. baeticum	Ebb07	Sierra Nevada, Almería, Spain	2128	37°05′46″N, 3°01′01″W	Purple	
	Ebb10	Sierra Nevada, Almería, Spain	2140	37°05′32″N, 3°00′40″W	Purple	En12
	Ebb12	Sierra Nevada, Almería, Spain	2264	37°05′51″N, 2°58′06″W	Purple	
E. bastetanum	Ebt01	Sierra de Baza, Granada, Spain	1990	37°22′52″N, 2°51′49″W	Purple	
	Ebt12	Sierra de María, Almería, Spain	1528	37°41′03″N, 2°10′51″W	Purple	
	Ebt13	Sierra Jureña, Granada, Spain	1352	37°57′10″N, 2°29′24″W	Purple	Em71
E. fitzii	Ef01	Sierra de la Pandera, Jaén, Spain	1804	37°37′56″N, 3°46′46″W	Yellow	
E. lagascae	Ela07	Sierra de San Vicente, Toledo, Spain	516	44°05′49″N, 4°40′40″W	Purple	
E. mediohispanicum	Em21	Sierra Nevada, Granada, Spain	1723	37°08′04″N, 3°25′43″W	Yellow	
	Em39	Sierra de Huétor, Granada, Spain	1272	37°19′08″N, 3°33′11″W	Yellow	Ep20
	Em71	Sierra Jureña, Granada, Spain	1352	37°57′10″N, 2°29′24″W	Yellow	Ebt13
E. nevadense	En05	Sierra Nevada, Granada, Spain	2074	37°06′35″N, 3°01′32″W	Yellow	
	En10	Sierra Nevada, Granada, Spain	2321	37°06′37″N, 3°24′18″W	Yellow	
	En12	Sierra Nevada, Granada, Spain	2255	37°05′37″N, 2°56′19″W	Yellow	Ebb10
E. popovii	Ep16	Jabalcuz, Jaén, Spain	796	37°45′26″N, 3°51′02″W	Purple	
	Ep20	Sierra de Huétor, Granada, Spain	1272	37°19′08″N, 3°33′11″W	Purple	Em39
	Ep27	Llanos del Purche, Granada, Spain	1470	37°07′46″N, 3°28′48″W	Purple	

Legend:
- ▼ *E. baeticum* (Ebb)
- ● *E. bastetanum* (Ebt)
- ○ *E. fitzii* (Ef)
- ■ *E. lagascae* (Ela)
- □ *E. mediohispanicum* (Em)
- ▽ *E. nevadense* (En)
- ● *E. popovii* (Ep)

FIG. 1. Map of the Iberian Peninsula showing the location of the sampled populations. The insert shows a more detailed map of the Baetic Mountains. Purple species are represented with purple symbols and yellow species are represented with yellow symbols. The populations Ebt13–Em71, Ebb10–En12 and Em39–Ep27 represent population pairs located in sympatry.

(yellow corollas; Em21, Em39 and Em71), *E. nevadense* (yellow corollas; En05, En10 and En12), *E. popovii* (purple corollas; Ep16, Ep20 and Ep27), *E. bastetanum* (purple corollas; Ebt01, Ebt12 and Ebt13) and *E. baeticum* (purple corollas; Ebb07, Ebb10 and Ebb12), and one population for *E. fitzii* (yellow corollas; Ef01). Some of these species appear in sympatry in some of the sampled localities (e.g. *E. popovii*, Ep20, and *E. mediohispanicum*, Em39; Table 1). Additionally, we sampled one population of *E. lagascae* (Ela07), an allopatric diploid species with purple corollas inhabiting Central Spain, posited as one potential parental species of the Baetic Mountain species studied here (Nieto-Feliner, 1993). We collected fully developed flower buds for transcriptomic analyses (five buds from an individual per population) and leaves for flow cytometry (6–10 individuals per population).

Flow cytometry analyses

We used flow cytometry to assess genome size and estimate DNA ploidy levels. Nuclei were isolated from fresh leaf tissues by simultaneously chopping with a razor blade 0.5 cm^2 of leaf and 0.5 cm^2 of an internal reference standard (Galbraith *et al.*, 1983). We used *Solanum lycopersicum* L. 'Stupické' with 2C = 1.96 pg or *Raphanus sativus* L. with 2C = 1.11 pg as internal reference standards (Doležel *et al.*, 1992). The extraction of nuclei was carried out on a Petri dish containing 1 mL of WPB buffer (Loureiro *et al.*, 2007). Then, the nuclear suspension was filtered using a 50 µm nylon mesh, and DNA was stained with 50 µg mL^{-1} of propidium iodide (PI; Fluka, Buchs, Switzerland). Additionally, 50 µg mL^{-1} of RNase (Fluka) was added to degrade double-stranded RNA (dsRNA). After a 5 min incubation, the samples were analysed in a Sysmex CyFlow Space flow cytometer (532 nm green solid-state laser, operating at 30 mW). Results were acquired using FloMax software v2.4d (Partec GmbH, Münster, Germany) in the form of four graphics: histogram of fluorescence pulse integral in linear scale (FL); forward light scatter (FS) vs. side light scatter (SS), both in logarithmic (log) scale; FL vs. time; and FL vs. SS in log scale. The FL histogram was gated using a polygonal region defined in the FL vs. SS histogram to avoid debris signals. At least 5000 particles were analysed per sample. Only coefficient of variation (CV) values of 2C peak of each sample below 5 % were accepted; otherwise, a new sample was prepared and

analysed until quality standards were achieved (Greilhuber *et al.*, 2007). In a few cases, samples produced histograms of poorer quality even after repetition due to the presence of cyto-solic compounds. Thus, it was impossible to estimate ploidy level and/or genome size for some samples (Table 2).

We obtained the genome size in mass units (2C in pg; *sensu* Greilhuber *et al.*, 2005) using the formula: sample 2C nuclear DNA content (pg) = (sample G_1 peak mean/reference standard G_1 peak mean) × genome size of the reference. The ploidy levels were inferred for each sample based on chromosome counts and genome size estimates available for the genus and species (Blanca *et al.*, 1992).

RNA extraction and sequencing

Details of the sampling, RNA extraction and sequencing appear in Osuna-Mascaró *et al.* (2021). In summary, we stored collected flower buds of each individual in liquid nitrogen until RNA extraction. Floral buds were ground with a mortar and a pestle in liquid nitrogen. We used the Qiagen RNeasy Plant Mini Kit following the manufacturer's protocol to isolate total RNA from 17 samples (one individual per population; three populations of *E. baeticum*, *E. bastetanum*, *E. mediohispanicum*, *E. nevadense* and *E. popovii*, and one population of *E. fitzii* and *E. lagascae*). Then, we checked the quality and quantity of the RNA using a NanoDrop 2000 spectrophotometer (Thermo Fisher Scientific, Wilmington, DE, USAs) and agarose gel electrophoresis. Library preparation and RNA sequencing were conducted at Macrogen Inc. (Seoul, Korea). Before sequencing, the quality of the RNA was analysed again with the Agilent 2100 Bioanalyzer system (Agilent Technologies Inc., Santa Clara, CA, USA), and an rRNA depletion procedure with Ribo-Zero (Illumina, San Diego, CA, USA) was used to enrich mRNA content and to avoid the sequencing of rRNA. Library preparation was performed using the TruSeq Stranded Total RNA LT Sample Preparation Kit (Plant). Sequencing of the 17 libraries (one per individual) was carried out using the Hiseq 3000–4000 sequencing protocol and TruSeq 3000–4000 SBS Kit v 3 reagent, following a paired-end 150 bp strategy on the Illumina HiSeq 4000 platform. A summary of sequencing statistics is shown in Supplementary data Table S1.

Transcriptome assembly and annotation

Details of the read quality control, trimming and *de novo* transcriptome assembly and annotation can be found in Osuna-Mascaró *et al.* (2021). Briefly, we used FastQC v0.11.5 (Andrews, 2010) to analyse the quality of each library's raw reads. Then, we trimmed the adaptors in the raw reads using cutadapt v1.15 (Martin, 2011), and we quality-filtered the reads using Sickle v1.33 (Joshi and Fass, 2011). After trimming, we used FastQC v0.11.5 (Andrews, 2010) again to verify the trimming efficiency. To assemble the resulting high-quality, cleaned reads into contigs, we followed a *de novo* approach using Trinity v 2.8.4 (Grabherr *et al.* 2011). Before assembly, each library was normalized *in silico* to validate and reduce the number of reads using the 'insilico_read_normalization.pl' function in Trinity (Haas *et al.*, 2013). Then we used the parameter 'min_kmer_cov 2' to eliminate single occurrence k-mers heavily enriched in sequencing errors, following Haas *et al.* (2013). Candidate open reading frames (ORFs) within transcript sequences were predicted and translated using TransDecoder v 5.2.0 (Haas *et al.*, 2013). We performed functional annotation of Trinity transcripts with ORFs using Trinotate v 3.0.1 (Haas, 2015). Sequences were searched against UniProt (UniProt Consortium, 2014), using the SwissProt databases (Bairoch and Apweiler, 2000) (with BLASTX and BLASTP searching and an e-value cut-off of 10^{-5}). We also used the Pfam

TABLE 2. *Genome size estimates and DNA ploidy levels obtained in populations of* Erysimum

Species	Population	DNA ploidy level		Genome size (2C, pg)					
		2n	*N*	Mean	s.d.	CV	Min	Max	*N*
E. baeticum	Ebb07	8*x*	5	2.08	0.08	3.85	1.93	2.17	2
	Ebb10	8*x*	6	2.07	0.09	4.35	1.93	2.17	5
	Ebb12	8*x*	–	–	–	–	–	–	–
E. bastetanum	Ebt01	4*x*	4	1.06	0.06	5.66	0.97	1.10	4
	Ebt12	4*x*	2	1.06	0.12	11.32	0.97	1.15	2
	Ebt13	8*x*	64	1.96	0.06	3.06	1.87	2.17	60
E. fitzii	Ef01	2*x*	3	0.44	0.004	0.91	0.44	0.45	3
E. lagascae	Ela07	2*x*	10	0.46	0.02	4.35	0.44	0.50	10
E. mediohispanicum	Em21	2*x*	2	0.44	0.01	2.27	0.43	0.44	2
	Em39	2*x*	21	0.46	0.02	4.35	0.43	0.49	19
	Em71	4*x*	59	0.98	0.04	4.08	0.93	1.13	59
E. nevadense	En05	2*x*	–	–	–	–	–	–	–
	En10	2*x*	–	–	–	–	–	–	–
	En12	2*x*	3	0.45	0.03	6.67	0.42	0.47	3
E. popovii	Ep16	4*x*	3	0.98	0.02	2.041.86	0.95	1.00	3
	Ep20	10*x*	15	2.49	0.06	2.416	2.40	2.60	10
	Ep27	4*x*	39	0.96	0.04	4.17	0.92	1.05	9

The following data are given for each population and ploidy level: mean, the standard deviation of the mean (s.d.), coefficient of variation (CV, %), minimum (Min) and maximum values (Max) of the holoploid genome size (2C, pg) followed by sample size for genome size estimates (*N*); DNA ploidy level (*2n*) and respective sample size (*N*) for ploidy estimates. DNA ploidy levels: 2*x*, diploid; 4*x*, tetraploid; 8*x*, octoploid; 10*x*, decaploid. For Ebb12, En05 and En10, samples it was not possible to estimate the ploidy levels, and we have used those described in Blanca *et al.* (1992).

database (Bateman *et al.*, 2004) to annotate protein domains for each predicted protein sequence. Transcripts were filtered through the eggnog (Jensen *et al.*, 2007), GO (Gene Ontology Consortium, 2004) and KEGG (Kanehisa and Goto, 2000) annotation databases.

Variant calling

We first ran a variant calling analysis, using the *E. lagascae* transcriptome as a reference. We indexed the *E. lagascae* transcriptome using BWA v 0.7.17 (Li and Durbin, 2009) to create a reference and then mapped all the trimmed raw reads to it using the BWA v 0.7.17 'mem' option (see Supplementary data Table S1 for mapping details). We used SAMtools v 1.7 (Li *et al.*, 2009) to convert and sort the alignment files. We then called single nucleotide polymorphisms (SNPs) using the SAMtools v 1.7 'mpileup' command. Lastly, we used bcftools v 1.9 to filter the SNPs (Narasimhan *et al.*, 2016), running the SAMtools v 1.7 Perl script 'vcfutils.pl VarFilter' with default parameters to filter down the candidate variants and to eliminate false positives.

Orthology inference

To reduce redundancy, we clustered the translated sequences using cd-hit v 4.6 (Li and Godzik, 2006), following the steps of the pipeline described in Yang and Smith (2014). For the inference of orthologues, we excluded untranslated regions (UTRs) and non-coding transcripts, using only coding DNA sequences (CDS) in order to avoid the inclusion of sequencing errors (Yang and Smith, 2014). We identified orthologue genes using the OrthoFinder v 2.3.3 pipeline (Emms and Kelly, 2015). In brief, this pipeline first made a BLASTP analysis with the protein sequences as input for searching the orthogroups (a set of potentially orthologous protein-coding genes derived from a single gene in the last common ancestor of all the species sampled), then clustered and aligned the orthologous sequences using MAFFT v 7.450 (Katoh and Standley, 2013) with default parameters. Finally, we obtained the maximum likelihood phylogenetic gene trees for all orthogroups using IQ-Tree v 1.6.1 (Nguyen *et al.*, 2014). Then, each orthogroup that contained sequences from all sampled species was used to infer a species tree using STAG v 1.0.0 (Emms and Kelly, 2019). Then, we used DLCpar v 1.1 (Wu *et al.*, 2014) to reconcile the species tree with the gene trees, considering gene duplication, losses and incomplete lineage sorting (ILS) as potential causes of discordance among trees.

Phylogenetic reconstruction

We obtained a coalescent species tree using ASTRAL v 5.6.3 (Mirarab *et al.*, 2014) with default parameters. This method reconstructs a species tree from unrooted gene tree topologies. We used the gene trees previously obtained by maximum likelihood by using IQ-Tree v 1.6.1 as input. We used FigTree v 1.4.0 (Rambaut and Drummond, 2012) to visualize and edit the species tree. Then, we compared the alternative tree topologies

with the phylogeny obtained from whole-chloroplast genome analyses for the same species (presented in Osuna-Mascaró *et al.*, 2021) using the Shimodaira–Hasegawa test (SH test; Shimodaira and Hasegawa, 1999) from the R package phangorn v 2.5.5 (Schliep, 2011). Both phylogenies were also compared visually, plotting them as mirror images with the function cophyloplot, using the R package ape v 5.4 (Paradis *et al.*, 2004).

Discriminant analysis of principal components

We conducted a discriminant analysis of principal components (DAPC; Jombart *et al.*, 2010) of the SNP data to group the different genotypes avoiding any prior subjective bias using the R package adegenet v 2.1.3 (Jombart and Ahmed, 2011). DAPC is a multivariate method that identifies and describes clusters of genetically related individuals from large datasets, providing a measure of the optimal number of genetic clusters (K) across a range of K values by using the Bayesian information criterion (BIC). We set a range of K values from two to seven since K = 7 is the number of different species in our dataset. The existence of significant hybridization and introgression would result in K < 7. To identify the optimal number of K, we selected the model with the lowest BIC.

Phylogenetic inference of introgression

As a first step to detect introgression events between species pairs, we computed phylogenetic species networks. This approach provides a graphical extension of the phylogenetic tree model, representing the gene flow by edges connecting the operational taxonomic units (OTUs) that are likely to be linked by introgression. We used the software PhyloNet v 3.6.9 (Than *et al.*, 2008; Wen *et al.*, 2018), which implements a phylogenetic network method based on the frequencies of rooted trees accounting for ILS. To generate the input for PhyloNet, we first ultrametricized the trees obtained previously with IQ-Tree v 1.6.1, using the 'nnls' method in the 'force.ultrametric' function within the R package phytools v 0.6-99 (Revell, 2012). Due to computational limitations, we inferred the species networks using a maximum pseudo-likelihood (MPL) method (Yu and Nakhleh, 2015). We performed the search five times to avoid getting stuck at local optima. We estimated optimal networks among an optimal computational range of 0–15 introgression events, determining the most likely network based on Akaike's information criterion (AIC; Bozdogan, 1987) with the generic function for AIC in R package stats v 3.6.1. As AIC may not provide precise values when using pseudo-likelihood phylogenetic networks (Cao *et al.*, 2019), we also estimated the more optimal network by slope heuristic of log-likelihood values. The optimal network was then visualized with Dendroscope v 3.5.10 (Huson and Scornavacca, 2019).

ABBA–BABA statistic

To assess gene flow between species, we calculated D-statistics, also known as the ABBA–BABA statistic (Durand

et al., 2011). To evaluate introgression among the seven species, we used the software Dsuite v 0.1 (Malinsky *et al.*, 2021), which allows the assessment of gene flow across large datasets and directly from a variant call format (VCF) file. This algorithm computes the D statistic by considering multiple groups of four populations: P1, P2, P3 and O, grouped in asymmetric trees of the form {[(P1, P2), P3], O}. The site patterns are ordered such that the pattern BBAA refers to P1 and P2 sharing the derived allele (B-derived allele, A-ancestral allele), ABBA to P2 and P3 sharing the derived allele and BABA to P1 and P3 sharing the derived allele. The ABBA and BABA patterns are expected to occur with equal frequencies, assuming no gene flow (null hypothesis), while a significant deviation from that suggests possible introgression. To assess whether D is significantly different from zero, D-suite uses a standard block-jackknife procedure (Green *et al.*, 2010; Durand *et al.*, 2011), obtaining approximately normally distributed standard errors. As recommended by Malinsky *et al.* (2021), we used a conservative approach estimating the statistic Dmin, which gives the lowest D-statistic value in a given trio. We used the ruby script 'plot_d.rb' to plot into a heatmap the introgression among all the pairs of samples. To complement these analyses, we computed the Fbranch statistic implemented in Dsuite v 0.1 (Malinsky *et al.*, 2018, 2021). The statistic allows the identification of gene flow events within specific internal branches of a phylogeny. Thus, evaluating the excess sharing of alleles between one species and the descendant or ancestral species helps to understand when the gene flow happened. We used the whole-chloroplast genomes phylogeny from Osuna-Mascaró *et al.* (2021) in Newick format to establish a reference phylogeny and specify which species could be more accurately treated as sister species (i.e. as P1 and P2) while always using *E. lagascae* as an outgroup.

Pollen tube growth

The existence of pre-zygotic barriers can fully impede interspecific hybridization. Therefore, the existence of such barriers may indicate that gene flow across a given set of species is highly unlikely, while the lack of such barriers may indicate plausible hybridization and introgression. To explore the existence of pre-zygotic barriers, we carried out a preliminary experiment on the growth of pollen tubes on a reduced set of co-occurring species (Table 1). We collected 20 individual plants each of *E. mediohispanicum*, *E. bastetanum* and *E. popovii* from natural populations. We grew the plants in a common garden (University of Granada facilities) and moved them into a greenhouse before flowering to exclude pollinators. When the flowers opened, we performed hand pollination experiments by tipping the anther with a small stick to remove the pollen and placing it on the stigma of a flower from different species previously emasculated (hybrid crosses) or of a flower from the same species but from different populations previously emasculated (intraspecific crosses). Moreover, we emasculated some flowers and hand-pollinated them with their own pollen (forced selfing crosses), and some flowers were not manipulated and left for spontaneous self-pollination (spontaneous selfing crosses). We collected the pistils after 72 h and preserved them in ethanol at 4 °C until staining of pollen tubes, following the

protocol of Mori *et al.* (2006) with minor modifications. In brief, each pistil was cleaned in 70 % ethanol (EtOH) for 10 min and then moved to 50 % EtOH, 30 % EtOH and finally distilled water. We softened the samples by placing them on a small Petri dish of 8 M NaOH for 1 h at room temperature (as recommended by Kearns and Inouye, 1993). Then, we transferred the pistils to distilled water for 10 min, and afterwards the stigmas were incubated with 0.1 % aniline blue in phosphate buffer (pH 8.3) for 2 h. The final slide preparations were examined under a fluorescence microscope with blue light (410 nm) to observe and measure pollen tube development.

RESULTS

Ploidy levels

Flow cytometry revealed a wide variation in genome size and, therefore, in DNA ploidy levels across but also within species (Table 2). We found that all samples of *E. fitzii* and *E. nevadense* were diploid. The other species with yellow corollas, *E. mediohispanicum*, also appeared to be predominantly diploid, although the Em71 population deviated from this pattern, being tetraploid. The genome size of *E. lasgacae* also corresponded to that of a diploid, while the other purple corolla species showed ploidy levels higher than diploidy (Table 2). Moreover, ploidy levels differed across populations in two of these species. Populations of *E. bastetanum* varied between 4*x* and 8*x*, while in *E. popovii* the range was even greater, from 4*x* to 10*x*. In three cases (Ebb12, En05 and En10; Table 2), it was not possible to establish the ploidy level of the samples, and we used those reported in Blanca *et al.* (1992).

Transcriptome assembly and orthology inference

The sequencing results and the corresponding summary statistics of the assembled transcriptomes can be found in Osuna-Mascaró *et al.* (2021). In summary, we obtained between 104 000 and 382 000 different Trinity transcripts, producing between 66 000 and 235 000 Trinity isogenes. The total assembled bases ranged from 92 Mbp (in the Em21 population of *E. mediohispanicum*) to 319 Mbp (in the En10 population of *E. nevadense*). The number of annotated unigenes ranged between 71 606 (*E. nevadense*, En12) and 197 069 (*E. baeticum*, Ebb10); mean value 146 314.35. The highest proportion of annotated unigenes was obtained using BLASTX to search against the SwissProt reference database. Details of the annotated unigenes using different protein databases can be found in Osuna-Mascaró *et al.* (2021). OrthoFinder assigned 1 519 064 protein gene sequences (96.4 % of the total) to 92 984 gene families (orthogroups) (Supplementary data Table S2). Among them, 16 941 orthogroups were shared by all species, and their corresponding gene trees were used for further analyses.

Phylogenetic trees and population clustering

We inferred a coalescence tree using the 16 941 maximum likelihood gene trees obtained with IQ-Tree as input for ASTRAL

(Fig. 2; Supplementary data Figs S1 and S2). This species tree was nearly fully resolved with high support, having only four nodes with low quartet scores results (posterior probabilities for these nodes: 0.78, 0.77, 0.70 and 0.53; see Supplementary data Fig. S1). In this tree, rooted with *E. lagascae*, the 4*x* population of *E. mediohispanicum* (yellow corollas; Em71) appeared as the first branching OTU. Three clades, although with low support, were evident. A clade was formed by *E. bastetanum* and *E. baeticum*, both species having purple corollas; another clade included *E. fitzii* (yellow corollas) and the three populations of *E. popovii* (purple corollas); and the last clade included the populations of *E. nevadense* and the 2*x* populations of *E. mediohispanicum*, both species with yellow corollas. Although there is some species clustering, not all species appear to be monophyletic, supporting a history of hybridization. Moreover, when comparing the species tree with the whole-chloroplast genomes phylogeny (Fig. 2), we find clear cytonuclear discordances resulting in a significant SH test result (Diff –ln L = 345 426.4, *P*-value < 0.01). This lack of congruence among both phylogenies also supports the hybridization hypothesis.

The discriminant analysis revealed K = 4 and K = 5 as the most likely number of genetic clusters (Fig. 3), both with very similar BIC values (K = 4, BIC = 189.99; K = 5, BIC = 188.99). The clusters corresponding to K = 4 produced the same clusters that appeared in the coalescence tree (Fig. 2). However, the clusters corresponding to K = 5 included three monospecific groups (for *E. lagascae*, purple corollas; *E. fitzii*, yellow corollas; and *E. popovii*, purple corollas), one for the diploid species with yellow corollas (the three populations of *E. nevadense* and the diploid populations of *E. mediohispanicum*) and the last including all the populations of *E. baeticum* (purple corollas), *E. bastetanum* (purple corollas), *E. popovii* (purple corollas) and Em71, the 4*x* population of *E. mediohispanicum* (yellow corollas).

Analysis of introgression

The network with 13 reticulation instances appeared as the most reliable based on the AIC values for the log-likelihood
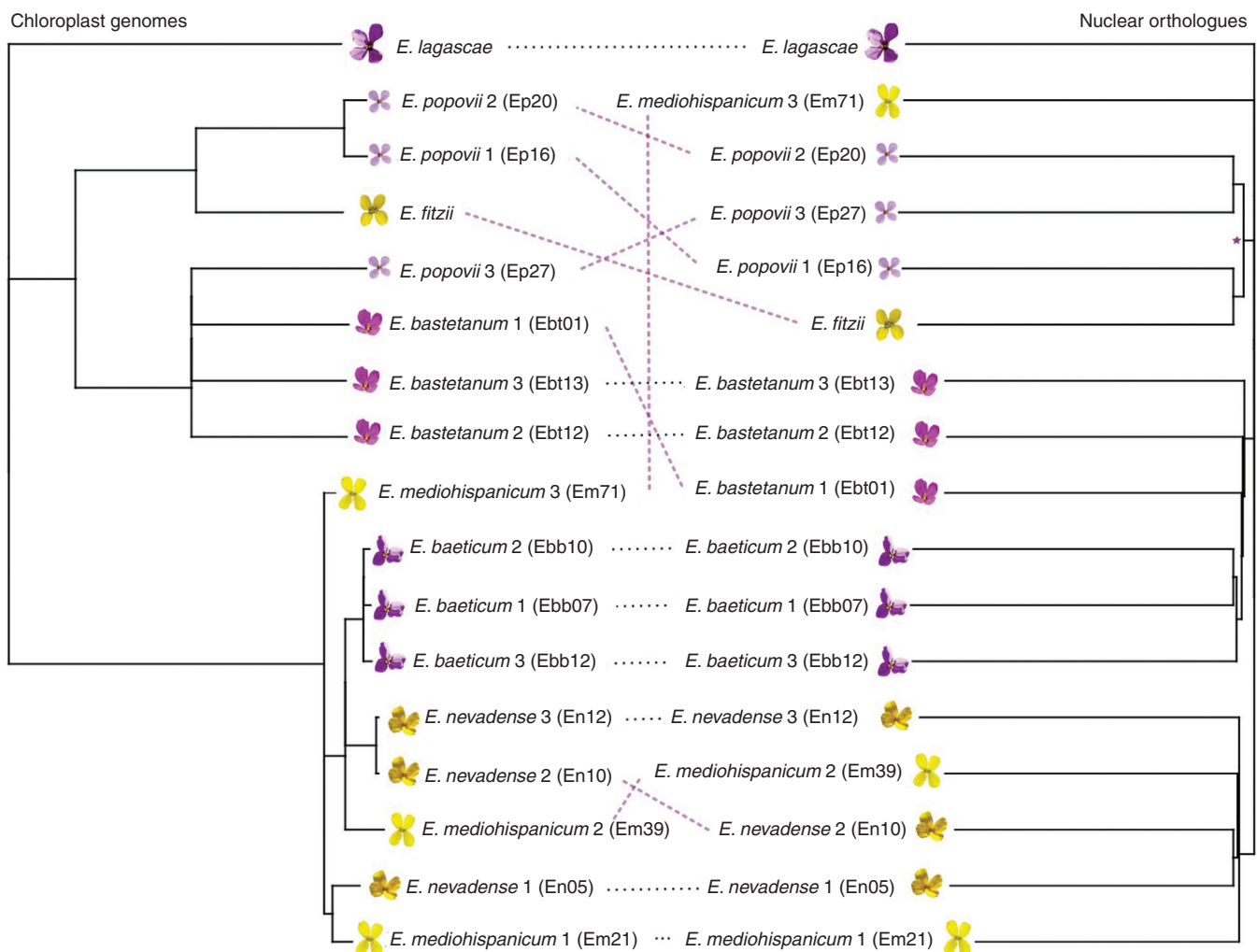

FIG. 2. Cyto-nuclear discordance in *Erysimum* spp. The phylogeny on the left was obtained using whole plastid genomes in Osuna-Mascaró *et al.* (2021). The phylogeny on the right is a representation of nuclear genome evolution and was generated from the 16 941 maximum likelihood gene trees computed using the SNP data described in the present paper (see text for details).
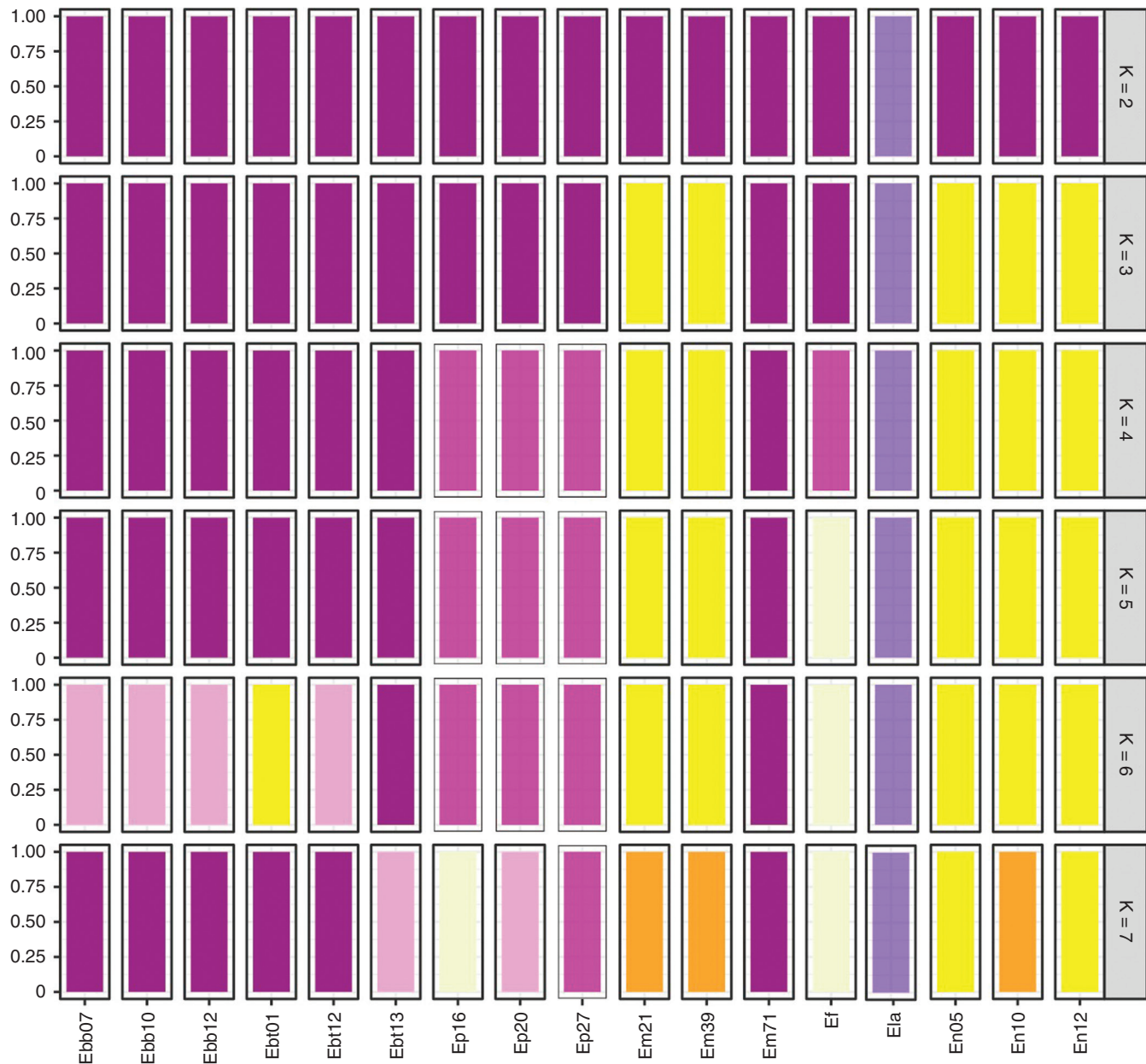
FIG. 3. Membership probability plot showing the DAPC results representing the populations grouped into pre-determined different clusters (ranging from K = 2 to K = 7, where each colour represents a cluster). The Bayesian analyses (BIC) revealed K = 5 as the most likely number of genetic clusters.

of the networks (Supplementary data Table S3). The estimates of the slope heuristic of log-likelihood values also supported the network with 13 reticulation instances as the most reliable network estimated. This network shows frequent hybridization events in the genealogy of these populations involving yellow and purple species (Fig. 4), as indicated by the edges connecting tree branches between different populations and species. Notably, this network includes edges connecting non-terminal branches (see Fig. 4), which indicates reticulations with past extinct taxa (i.e. 'ghost species') or incomplete sampled taxa.

The ABBA–BABA analyses support this scenario of frequent hybridization, even using a conservative approach (D-min). We summarized the tested topologies and the inferred D-statistics with corrected *P*-values for all triplet combinations in Supplementary data Table S4 and Fig. S3. The highest signal

of introgression occurred between *E. fitzii* (yellow corollas) and *E. baeticum* (purple corollas; populations Ebb12 and Ebb10) and *E. popovii* (purple corollas; Ep16); and between *E. popovii* (purple corollas; Ep16) and *E. bastetanum* (purple corollas; Ebt12) and *E. baeticum* (purple corollas; Ebb07, Ebb10 and Ebb12). There was also evidence of interspecific gene flow as manifested by the fbranch statistic (Supplementary data Fig. S4) that identifies gene flow events into specific internal branches of the phylogeny while accounting for potential false-positive results due to correlated introgression signatures among closely related species. Specifically, we found the highest signal of gene flow between *E. bastetanum* (purple corollas; Ebt12) and *E. mediohispanicum* (yellow corollas; Em71 and Em21), *E. nevadense* (yellow corollas; En12 and En05) and *E. baeticum* (purple corollas; Ebb07 and Ebb10); between
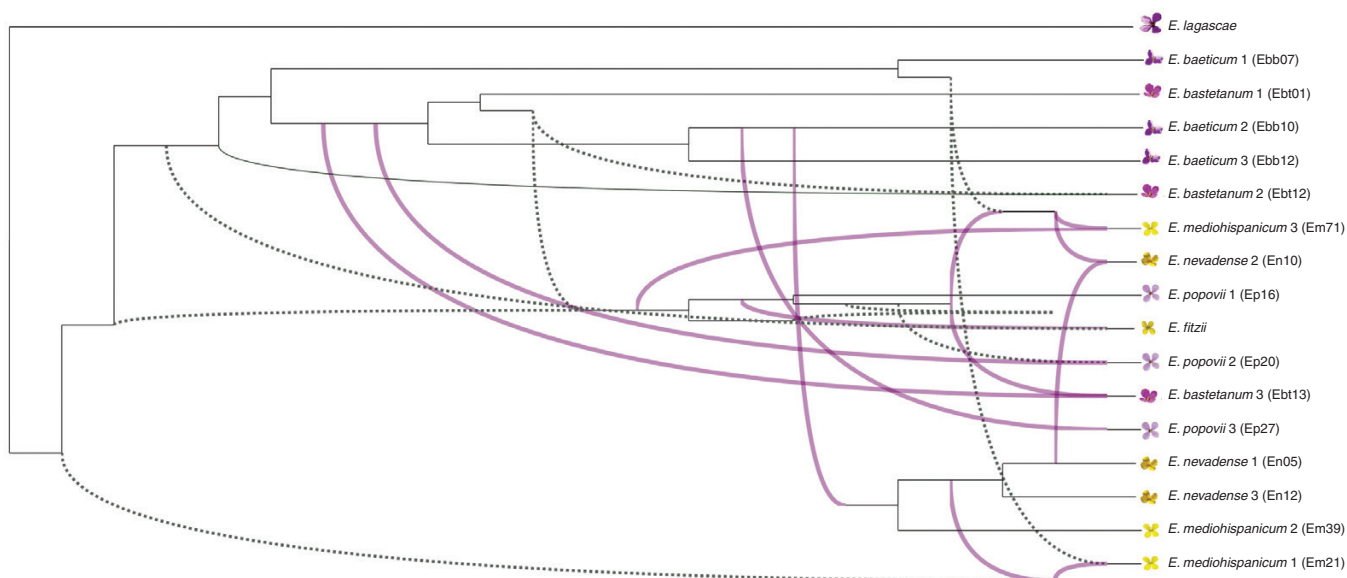
FIG. 4. Optimal species network. The graph represents a maximum pseudo-likelihood (MPL) tree with 13 reticulations computed using PhyloNet. These events are represented by edges connecting the tree branches between different individuals and indicate likely hybridization between different taxa. Note that in some instances, introgression appears to involve ancestral or extinct taxa (i.e. ghost species, dotted lines).

E. bastetanum (purple corollas; Ebt13) and *E. mediohispanicum* (yellow corollas; Em71) and *E. popovii* (purple corollas; Ep20); and between *E. bastetanum* (purple corollas; Ebt01) and *E. mediohispanicum* (yellow corollas; Em21 and Em39) and *E. nevadense* (yellow corollas; En12). In addition, we have detected other gene flow events with ancestral or non-sampled taxa (Supplementary data Fig. S4).

Pollen tube growth

A total of 103 preparations of *Erysimum* pistils were examined: 52 from hybrid crosses, 24 from forced selfing crosses, 16 from spontaneous selfing crosses and 11 from intraspecific crosses (Supplementary data Table S5). Our results showed full growth of pollen tubes (i.e. reaching the ovary) in 63.33 % of intraspecific crosses, 51.92 % of hybrid crosses ($\chi^2 = 0.50$, *P*-value = 0.513 compared with intraspecific crosses), only in 29.16 % of forced selfing crosses ($\chi^2 = 3.73$, *P*-value = 0.074) and in 25.16 % of spontaneous selfing crosses ($\chi^2 = 4.03$, *P*-value = 0.057). Although these last values were not significant, when selfing classes were pooled, a significant reduction in the growth of pollen tubes was shown ($\chi^2 = 4.93$, *P*-value = 0.039) (Supplementary data Fig. S5). Cases in which pollen tubes grew but did not reach the ovary were treated as non-growing. In these cases, we could not estimate whether tube growth had completely stopped or if it was ongoing but developed too slowly to reach the ovary during the duration of the experiment.

DISCUSSION

Our results suggest that the *Erysimum* species studied here have a strong signature of hybridization and introgression in their genomes. This result is supported by the pollen tube growth experiments that showed that pollen tubes could grow all the way to the ovary in some hybrid crosses, indicating very weak or non-existent pre-zygotic barriers. Moreover, we found that species with purple flowers are polyploid and have a strong signature of introgression, suggesting an allopolyploid origin. We also found a hybridization signature in the (mostly diploid) yellow species, indicating that hybridization occurred across both colours and ploidy levels.

Several phylogenetic reconstructions have been performed for western Mediterranean *Erysimum* species (e.g. Abdelaziz *et al.* 2014; Gómez *et al.*, 2014, 2015*b*; Züst *et al.*, 2020) that have used different strategies (several populations per species or only one representative per species; several nuclear and cytoplasmic sequences; or next-generation sequencing transcriptomic data). Abdelaziz *et al.* (2014) found that populations of *E. mediohispanicum* and *E. bastetanum*, species analysed here, did not appear as monophyletic (with some populations placed within other branches of the phylogeny), which was indicative that introgression probably produced important reticulation at the population level. Our analyses support this hypothesis. The reticulate nature of these phylogenies imposes some caution in interpreting phylogenies based on only a few nuclear or cytoplasmic sequences, as suggested by Chan and Levin (2005). In these cases, major divisions may reflect the reality of some old phylogenetic splits. However, it will be challenging for more recent speciation events to provide a clear picture of the phylogeny without interrogating complete genomes or transcriptomes.

Overall, our results support a hybrid origin for the purple polyploid *Eysimum* Iberian species, as suggested in previous studies (Nieto-Feliner, 1993; Abdelaziz *et al.*, 2014; Gómez *et al.*, 2015*b*; Osuna-Mascaró, 2020). In particular, we found support for *E. popovii* (purple corollas and polyploid) and *E. fitzii* (yellow corollas and diploid) as sister species. Also, the genome of *E. popovii* exhibited signatures of a hybridization process in which *E. fitzii* may have been involved. The possible

hybrid origin of *E. popovii* with *E. fitzii* as a potential parental taxon was previously proposed by Nieto-Feliner (1993) based on morphology. Similarly, a hybrid origin of *E. baeticum* (purple corollas and polyploid) had been previously suggested, in this case with *E. nevadense* (yellow corollas and diploid) implicated as a potential parent (Nieto-Feliner, 1992). Our results showed that these two species appear to be closely related, and *E. baeticum* may have had an introgression signature of *E. nevadense*. Moreover, our results also suggested a complex scenario for *E. bastetanum* (purple corollas and polyploid), which appears closely related to *E. baeticum* (purple corollas and polyploid). In fact, *E. bastetanum* has been considered a subspecies of *E. baeticum* until recently (Lorite *et al.*, 2015). Therefore, the general pattern that emerged from our results is that these purple species are polyploids of hybrid origin, descending from crosses between an unidentified parent and some diploid, often yellow taxon.

However, our results also suggested a complex evolutionary history for the mostly diploid yellow species. The contributing lineages also often involve unidentified taxa. This might be attributable to insufficient sampling, as we did not include some *Erysimum* species (*E. rondae* and *E. myriophyllum*, yellow corollas; and *E. cazorlense*, purple corollas) that also inhabit the Baetic Mountains, although with a limited distribution (Nieto-Feliner, 1993). At this point, it is impossible to establish whether these taxa may have acted as a source of introgression. In any case, our results show that hybridization and introgression are major contributors to the evolutionary history of this species complex, deserving further research.

Interestingly, we did not find a consistent, predictable pattern of hybridization for most species. Populations of the same species showed differences in their hybridization history, as demonstrated by the ABBA–BABA test (which detected multiple and diverse introgression events) and the PhyloNet reconstructions (which yielded a tree with 13 reticulations as the most optimal network). In the same vein, the DAPC results did not support a scenario with populations clustered by species. Our results are similar to those of previous studies describing asymmetric hybridization patterns as a consequence of differences in ecological pressures across populations and geographical areas (Payton *et al.*, 2019; Sujii *et al.*, 2019; Wang *et al.*, 2019). At this stage, we cannot unambiguously identify any ecological factor behind the asymmetries we detected. However, we did observe variation in pollinators' preferences and flowering time across populations, which might lead to local differences in gene flow patterns (unpublished data). Thus, to fully understand this asymmetry in hybridization and why some populations have more introgression signatures than others, future studies considering different ecological pressures for these species and including pollinator censures of wild populations are required. Furthermore, it would also be interesting to conduct a functional analysis of the introgressed regions to establish clearly the metabolic routes affected by them. This information, coupled with detailed ecological studies, could throw light on the adaptive processes that foster genetic exchanges in this group.

Evidence of hybridization between at least some of these species has been reported previously (Abdelaziz *et al.*, 2014). Thus, *E. mediohispanicum* and *E. nevadense* show a hybrid zone in a sector of the Spanish Sierra Nevada (Abdelaziz *et al.*, 2021). Pollinators do not appear to constitute strong pre-pollinating barriers since all of these species are extreme generalists and share most pollinators (Gómez *et al.*, 2015b). Moreover, we have found that pre-zygotic, post-pollination barriers may not be effective since pollen tubes are often growing in hybrid crosses. Contemporary gene flow between different cytotypes of *E. mediohispanicum* seems negligible, as evidenced by an almost complete absence of triploids and other minority cytotypes in the contact zone between tetraploid and diploid populations of this species (Muñoz-Pajares *et al.*, 2018). Historical dynamics of genetic isolation and sympatry might have also played a role (Albaladejo and Aparicio, 2007; Rifkin *et al.*, 2019; Zieliński *et al.*, 2019). These *Erysimum* species are located in a well-known glacial refugium (Médail and Diadema, 2009; Hughes and Woodward, 2017), and thus the isolation and then re-establishment of gene flow (i.e. secondary contact zones) among populations of different species may have favoured locally specific hybridization patterns (Coyne and Orr, 2004; Harrison and Larson, 2014; Arnold, 2015). A better knowledge of the historical dynamics of species and populations and overlap of past ranges is required to fully understand the genomic pattern of divergence between closely related species. For instance, combining macroecological methods with niche models and phylogenetic approaches could clarify the opportunity for hybridization through evolutionary time (Folk *et al.*, 2018; Aguirre-Liguori *et al.*, 2021).

Furthermore, we detected signatures of ghost introgression, implying that ancestral species have influenced the hybridization history of these *Erysimum* species. This result was first evidenced by cytonuclear discordance, which might be due to past organellar introgression from extinct species (Huang *et al.*, 2014; Folk *et al.*, 2017; Lee-Yaw *et al.*, 2019). We also found a clear signature of ancestral introgression in the phylogenetic species network, in which some of the reticulations appeared from introgression involving 'ghost' taxa. Similarly, the fbranch statistic identified gene flow events in internal branches that concurred with introgression with ghost species. Specifically, we observed that some ancestral form of *E. popovii* (purple corollas and polyploid) could have been related to *E. fitzii* (yellow corollas and polyploid). Also, we detected evidence of gene flow between an ancestor of *E. mediohispanicum* (yellow corollas and diploid; Em21), *E. bastetanum* (purple corollas and polyploid) and *E. baeticum* (purple corollas and polyploid). Moreover, the results showed that many past gene flow events could have occurred between *E. baeticum* (purple corollas and polyploid), *E. nevadense* (yellow corollas and diploid) and *E. bastetanum* (purple corollas and polyploid). In light of these results, it seems that some unidentified ancestral species played a role as introgression sources for both the purple and yellow species. However, as previously noted, we include only a sub-set of the Iberian *Erysimum* species in this study; accordingly, we may be mistaking the signal of the unsampled species for that of ancestral taxa. Further research about the ghost introgression's influence on *Erysimum* evolution, including all the Iberian species and high-quality genome assemblies, would be required to thoroughly understand the hybridization history.

CONCLUSIONS

Our results indicate that complex evolutionary dynamics have shaped present-day Iberian *Erysimum* diversity. The genomes of extant taxa are the product of multiple polyploidizations,

hybridization and introgression events. Understanding these multifaceted processes and their interplay is crucial to characterize the evolution of *Erysimum* spp. and probably of angiosperms in general. Although the evolution of the Iberian *Erysimum* might have been particularly dynamic, this group could be representative of the evolutionary response of multispecies complexes to drastic environmental fluctuations. Further research that incorporates a wider taxonomic sample, whole-genome sequences and complex demographic and evolutionary statistical methods is needed to precisely characterize the patterns described here.

SUPPLEMENTARY DATA

Supplementary data are available online at https://academic. oup.com/aob and consist of the following.

Figure S1: phylogeny inferred after a species tree analysis of 16 941 gene trees. Figure S2: densitree plot based on 16 941 gene trees. Figure S3: heatmap depicting the introgression found by Dsuite. Figure S4: heatmap depicting the gene flow among phylogeny branches estimated with the fbranch statistic. Figure S5: pollen tube growth as a result of hand pollination crosses. Table S1: summary of sequencing and mapping statistics. Table S2: summary of OrthoFinder results. Table S3: log likelihood and AIC for all the estimated phylogenetic species network. Table S4: D-statistics with corrected *P*-values for all triplet combinations. Table S5: *Erysimum* pistil preparations.

DATA AVAILABILITY

Data are available in the NCBI Sequence Read Archive BioProject PRJNA607615 under the following accession numbers: *E. popovii*: Ep27 (SRX7756239), Ep20 (SRX7756238), Ep16 (SRX7756237); *E. lagascae*: Ela07 (SRX7756236); *E. fitzii*: Ef01 (SRX7756235); and *E. bastetanum*: Ebt13 (SRX7756233), Ebt12 (SRX7756232), Ebt01 (SRX7756231); and BioProject PRJNA473238 under the following accession numbers: *E. baeticum*: Ebb12 (SRX4130243), Ebb10 (SRX4130242), Ebb07 (SRX4130235); *E. mediohispanicum*: Em39 (SRX4130241), Em71 (SRX4130240), Em21 (SRX4130233); and *E. nevadense*: En12 (SRX4130237), En10 (SRX4130236), En05 (SRX4130234).

ACKNOWLEDGEMENTS

FUNDING

LITERATURE CITED

Abbott R, Albach D, Ansell S, *et al.* **2013.** Hybridization and speciation. *Journal of Evolutionary Biology* **26**: 229–246. doi:10.1111/j.1420-9101.2012.02599.x.

Abdelaziz M. 2013. *How species are evolutionarily maintained? Pollinator-mediated divergence and hybridization in Erysimum mediohispanicum and Erysimum nevadense*. PhD Thesis, Universidad de Granada, Spain.

Abdelaziz M, Muñoz-Pajares AJ, Lorite J, Herrador MB, Perfectti F, Gómez Reyes JM. 2014. Phylogenetic relationships of *Erysimum* (Brassicaceae) from the Baetic Mountains (SE Iberian peninsula). *Anales del Jardín Botánico de Madrid* **71**: e005.

Abdelaziz M, Muñoz-Pajares AJ, Berbel M, García-Muñoz A, Gómez JM, Perfectti F. 2021. Asymmetric reproductive barriers and gene flow promote the rise of a stable hybrid zone in the Mediterranean high mountain. *Frontiers in Plant Science* **12**: 687094. doi:10.3389/fpls.2021.687094.

Aguirre-Liguori JA, Ramírez-Barahona S, Gaut BS. 2021. The evolutionary genomics of species'responses to climate change. *Nature Ecology & Evolution* **5**: 1–11.

Albaladejo RG, Aparicio A. 2007. Population genetic structure and hybridization patterns in the Mediterranean endemics *Phlomis lychnitis* and *P. crinita* (Lamiaceae). *Annals of Botany* **100**: 735–746. doi:10.1093/aob/mcm154.

Anderson E. 1953. Introgressive hybridization. *Biological Reviews* **28**: 280–307. doi:10.1111/j.1469-185x.1953.tb01379.x.

Anderson E, Hubricht L. 1938. Hybridization in Tradescantia. III. The evidence for introgressive hybridization. *American Journal of Botany*: 396–402.

Andrews S. 2010. *FastQC: a quality control tool for high throughput sequence data*. http://www.bioinformatics.babraham.ac.uk/projects/fastqc/

Arnold ML. 2015. *Divergence with genetic exchange*. Oxford: Oxford University Press.

Arnold ML, Bulger MR, Burke JM, Hempel AL, Williams JH. 1999. Natural hybridization: how low can you go and still be important? *Ecology* **80**: 371–381. doi:10.1890/0012-9658(1999)080[0371:nhhlcy]2.0.co;2.

Bairoch A, Apweiler R. 2000. The SWISS-PROT protein sequence database and its supplement TrEMBL in 2000. *Nucleic Acids Research* **28**: 45–48. doi:10.1093/nar/28.1.45.

Bateman A, Coin L, Durbin R, *et al.* **2004.** The Pfam protein families database. *Nucleic Acids Research* **32**: D138–D141. doi:10.1093/nar/gkh121.

Blanca G, Torres MCM, Rejón MR. 1992. El género '*Erysimum*' L.('Cruciferae') en Andalucía (España). *Anales del Jardín Botánico de Madrid* **49**: 201–214.

Bozdogan H. 1987. Model selection and Akaike's information criterion (AIC): The general theory and its analytical extensions. *Psychometrika* **52**: 345–370. doi:10.1007/bf02294361.

Cao Z, Liu X, Ogilvie HA, Yan Z, Nakhleh L. 2019. Practical aspects of phylogenetic network analysis using phylonet. *BioRxiv*. doi:10.1101/746362. [Preprint].

Chan KM, Levin SA. 2005. Leaky prezygotic isolation and porous genomes: rapid introgression of maternally inherited DNA. *Evolution* **59**: 720–729.

Chapman MA, Abbott RJ. 2010. Introgression of fitness genes across a ploidy barrier. *New Phytologist* **186**: 63–71.

Coyne JA, Orr HA. 2004. *Speciation*. Sunderland, MA: Sinauer Associates.

Doležel J, Sgorbati S, Lucretti S. 1992. Comparison of three DNA fluorochromes for flow cytometric estimation of nuclear DNA content in plants. *Physiologia Plantarum* **85**: 625–631.

Durand EY, Patterson N, Reich D, Slatkin M. 2011. Testing for ancient admixture between closely related populations. *Molecular Biology and Evolution* **28**: 2239–2252. doi:10.1093/molbev/msr048.

Emms DM, Kelly S. 2015. OrthoFinder: solving fundamental biases in whole genome comparisons dramatically improves orthogroup inference accuracy. *Genome Biology* **16**: 157.

Emms DM, Kelly S. 2019. OrthoFinder: phylogenetic orthology inference for comparative genomics. *Genome Biology* **20**: 1–14.

Folk RA, Mandel JR, Freudenstein JV. 2017. Ancestral gene flow and parallel organellar genome capture result in extreme phylogenomic discord in a lineage of angiosperms. *Systematic Biology* **66**: 320–337. doi:10.1093/sysbio/syw083.

Folk RA, Visger CJ, Soltis PS, Soltis DE, Guralnick RP. 2018. Geographic range dynamics drove ancient hybridization in a lineage of angiosperms. *The American Naturalist* **192**: 171–187. doi:10.1086/698120.

Galbraith DW, Harkins KR, Maddox JM, *et al.* **1983.** Rapid flow cytometric analysis of the cell cycle in intact plant tissues. *Science* **220**: 1049–1051. doi:10.1126/science.220.4601.1049.

Gene Ontology Consortium. **2004.** The Gene Ontology (GO) database an informatics resource. *Nucleic Acids Research* **32**: D258–D261.

Gómez JM, Perfectti F, Klingenberg CP. 2014. The role of pollinator diversity in the evolution of corolla-shape integration in a pollination-generalist plant clade. *Philosophical Transactions of the Royal Society B: Biological Sciences* **369**: 1–11.

Gómez JM, González-Mejias A, Lorite J, Abdelaziz M, Perfectti F. 2015a. The silent extinction: climate change and the potential for hybridization-mediated extinction of endemic high-mountain plants. *Biodiversity and Conservation* **24**: 1843–1857.

Gómez JM, Perfectti F, Lorite J. 2015b. The role of pollinators in floral diversification in a clade of generalist flowers. *Evolution* **69**: 863–878. doi:10.1111/evo.12632.

Goulet BE, Roda F, Hopkins R. 2017. Hybridization in plants: old ideas, new techniques. *Plant Physiology* **173**: 65–78.

Grabherr MG, Haas BJ, Yassour M, *et al.* **2011.** Full-length transcriptome assembly from RNA-Seq data without a reference genome. *Nature Biotechnology* **29**: 644–652. doi:10.1038/nbt.1883.

Green RE, Krause J, Briggs AW, *et al.* **2010.** A draft sequence of the Neandertal genome. *Science* **328**: 710–722. doi:10.1126/science.1188021.

Greilhuber J, Doležel J, Lysak MA, Bennett MD. 2005. The origin, evolution and proposed stabilization of the terms 'genome size' and 'C-value' to describe nuclear DNA contents. *Annals of Botany* **95**: 255–260.

Greilhuber J, Temsch EM, Loureiro JC. 2007. Nuclear DNA content measurement. In: Dolezel J, Greilhuber J, Suda J, eds. *Flow cytometry with plant cells: analysis of genes, chromosomes and genomes*. Weinheim, Germany: Wiley, 67–101.

Greuter W, Burdet HM, Long G. 1986. Dicotyledones (Convolvulaceae-Labiatae). *Med-Checklist* **3**: 106–116.

Haas BJ. 2015. *Trinotate: transcriptome functional annotation and analysis*. https://trinotate.github.io/

Haas BJ, Papanicolaou A, Yassour D, *et al.* **2013.** De novo transcript sequence reconstruction from RNA-Seq using the Trinity platform for reference generation and analysis. *Nature Protocols* **8**: 1494.

Harrison RG, Larson EL. 2014. Hybridization, introgression, and the nature of species boundaries. *Journal of Heredity* **105**: 795–809. doi:10.1093/jhered/esu033.

Huang DI, Hefer CA, Kolosova N, Douglas CJ, Cronk QC. 2014. Whole plastome sequencing reveals deep plastid divergence and cytonuclear discordance between closely related balsam poplars, *Populus balsamifera* and *P. trichocarpa* (Salicaceae). *New Phytologist* **204**: 693–703.

Hughes PD, Woodward JC. 2017. Quaternary glaciation in the Mediterranean mountains: a new synthesis. *Geological Society London Special Publications* **433**: 1–23.

Huson DH, Scornavacca C. 2019. *User Manual for Dendroscope V 3.6.2.* https://software-ab.informatik.uni-tuebingen.de/download/dendroscope/manual.pdf

Jensen LJ, Julien P, Kuhn M, *et al.* **2007.** eggNOG: automated construction and annotation of orthologous groups of genes. *Nucleic Acids Research* **36**: D250–D254. doi:10.1093/nar/gkm796.

Jombart T, Ahmed I. 2011. adegenet 1.3-1: new tools for the analysis of genome-wide SNP data. *Bioinformatics* **27**: 3070–3071. doi:10.1093/bioinformatics/btr521.

Jombart T, Devillard S, Balloux F. 2010. Discriminant analysis of principal components: a new method for the analysis of genetically structured populations. *BMC Genetics* **11**: 94. doi:10.1186/1471-2156-11-94.

Joshi NA, Fass JN. 2011. *Sickle: a sliding-window, adaptive, quality-based trimming tool for FastQ files (Version1.33)* [Software]. https://github.com/najoshi/sickle

Kanehisa M, Goto S. 2000. KEGG: Kyoto Encyclopedia of Genes and Genomes. *Nucleic Acids Research* **28**: 27–30. doi:10.1093/nar/28.1.27.

Katoh K, Standley DM. 2013. MAFFT multiple sequence alignment software version 7: improvements in performance and usability. *Molecular Biology and Evolution* **30**: 772–780. doi:10.1093/molbev/mst010.

Kearns CA, Inouye DW. 1993. *Techniques for pollination biologists*. Niwot: University Press of Colorado.

Lee-Yaw JA, Grassa CJ, Joly S, Andrew RL, Rieseberg LH. 2019. An evaluation of alternative explanations for widespread cytonuclear discordance in annual sunflowers (*Helianthus*). *New Phytologist* **221**: 515–526.

Li H, Durbin R. 2009. Fast and accurate short read alignment with Burrows–Wheeler transform. *Bioinformatics* **25**: 1754–1760. doi:10.1093/bioinformatics/btp324.

Li H, Handsaker B, Wysoker A, *et al.* **2009.** The sequence alignment/map format and SAMtools. *Bioinformatics* **25**: 2078–2079. doi:10.1093/bioinformatics/btp352.

Li W, Godzik A. 2006. Cd-hit: a fast program for clustering and comparing large sets of protein or nucleotide sequences. *Bioinformatics* **22**: 1658–1659. doi:10.1093/bioinformatics/btl158.

Lorite J, Perfectti F, Gómez JM. 2015. A new combination in *Erysimum* (Brassicaceae) for Baetic mountains (South-eastern Spain). *Phytotaxa* **201**: 103–105. doi:10.11646/phytotaxa.201.1.10.

Loureiro J, Rodriguez E, Doležel J, Santos C. 2007. Two new nuclear isolation buffers for plant DNA flow cytometry: a test with 37 species. *Annals of Botany* **100**: 875–888.

Malinsky M, Svardal H, Tyers AM, *et al.* **2018.** Whole-genome sequences of Malawi cichlids reveal multiple radiations interconnected by gene flow. *Nature Ecology & Evolution* **2**: 1940–1919.

Malinsky M, Matschiner M, Svardal H. 2021. Dsuite-Fast D-statistics and related admixture evidence from VCF files. *Molecular Ecology Resources* **21**: 584–595. doi:10.1111/1755-0998.13265.

Mallet J. 2005. Hybridization as an invasion of the genome. *Trends in Ecology & Evolution* **20**: 229–237. doi:10.1016/j.tree.2005.02.010.

Marhold K, Lihová J. 2006. Polyploidy, hybridization and reticulate evolution: lessons from the Brassicaceae. *Plant Systematics and Evolution* **259**: 143–174. doi:10.1007/s00606-006-0417-x.

Martin M. 2011. Cutadapt removes adapter sequences from high throughput sequencing reads. *EMBnetJ* **17**: 10–12.

Mateo G, Villalba MBC, Udias SL. 1998. Acerca del orófito minusvalorado de la Sierra de Javalambre (Teruel). *Flora Montiberica* **9**: 41–45.

Mayr E. 1992. A local flora and the biological species concept. *American Journal of Botany* **79**: 222–238. doi:10.1002/j.1537-2197.1992.tb13641.x.

Médail F, Diadema K. 2009. Glacial refugia influence plant diversity patterns in the Mediterranean Basin. *Journal of Biogeography* **36**: 1333–1345. doi:10.1111/j.1365-2699.2008.02051.x.

Mirarab S, Reaz R, Bayzid MS, Zimmermann T, Swenson MS, Warnow T. 2014. ASTRAL: genome-scale coalescent-based species tree estimation. *Bioinformatics* **30**: i541–i548. doi:10.1093/bioinformatics/btu462.

Mori T, Kuroiwa H, Higashiyama T, Kuroiwa T. 2006. Generative Cell Specific 1 is essential for angiosperm fertilization. *Nature Cell Biology* **8**: 64–71. doi:10.1038/ncb1345.

Muñoz-Pajares AJ. 2013. *Erysimum mediohispanicum at the evolutionary crossroad: phylogeography, phenotype, and pollinators*. PhD Thesis, Universidad de Granada, Spain.

Muñoz-Pajares AJ, Perfectti F, Loureiro J, *et al.* **2018.** Niche differences may explain the geographic distribution of cytotypes in *Erysimum mediohispanicum*. *Plant Biology* **20**: 139–147.

Narasimhan V, Danecek P, Scally A, Xue Y, Tyler-Smith C, Durbin R. 2016. BCFtools/RoH: a hidden Markov model approach for detecting autozygosity from next-generation sequencing data. *Bioinformatics* **32**: 1749–1751. doi:10.1093/bioinformatics/btw044.

Nguyen LT, Schmidt HA, von Haeseler A, Minh BQ. 2014. IQ-TREE: a fast and effective stochastic algorithm for estimating maximum-likelihood phylogenies. *Molecular Biology and Evolution* **32**: 268–274. doi:10.1093/molbev/msu300.

Nieto-Feliner G. 1992. Los '*Erysimum*' orófilos nevadenses de flor amarilla y purpúreo-violácea: ¿son coespecíficos? *Anales del Jardín Botánico de Madrid* **50**: 272–274.

Nieto-Feliner G. 1993. *Erysimum* L. In: *Flora iberica. Vol. 4. Cruciferae-Monotropaceae*. Madrid: Real Jardín Botánico, 48–76.

Nieto-Feliner G. 2011. Southern European glacial refugia: a tale of tales. *Taxon* **60**: 365–372.

Osuna Mascaró C. 2020. *Hybridization as an evolutionary driver for speciation: a case in the Southern European Erysimum species*. PhD Thesis, Universidad de Granada, Spain.

Osuna-Mascaró C, Rubio de Casas R, Landis JB, Perfectti F. 2021. Genomic resources for *Erysimum* spp. (Brassicaceae): transcriptome and chloroplast genomes. *Frontiers in Ecology and Evolution* **9**: 206.

Paradis E, Claude J, Strimmer K. 2004. APE: analyses of phylogenetics and evolution in R language. *Bioinformatics* **20**: 289–290. doi:10.1093/bioinformatics/btg412.

Payseur BA, Rieseberg LH. 2016. A genomic perspective on hybridization and speciation. *Molecular Ecology* **25**: 2337–2360.

Payton AC, Naranjo AA, Judd W, Gitzendanner M, Soltis PS, Soltis DE. 2019. Population genetics, speciation, and hybridization in *Dicerandra* (Lamiaceae), a North American Coastal Plain endemic, and implications for conservation. *Conservation Genetics* **20**: 531–543. doi:10.1007/s10592-019-01154-8.

Polatschek A. 1978. Die arten der gattung *Erysimum* auf der Iberischen Halbinsel. *Annalen des Naturhistorischen Museums in Wien* **325**: 362.

Polatschek A. 1986. *Erysimum*. In: Strid A, ed. *Mountain flora of Greece*. Cambridge: Cambridge University Press, 239–247.

Polatschek A. 2014. Revision der gattung *Erysimum* (Cruciferae): Nachträge zu den bearbeitungen derIberischen. Halbinsel und Makaronesiens. *Annalen des Naturhistorischen Museums in Wien. Serie B für Botanik und Zoologie* **87**: 105.

Rambaut A, Drummond AJ. 2012. *FigTree version 1.4.0*. https://github.com/rambaut/figtree/

Revell LJ. 2012. phytools: an R package for phylogenetic comparative biology (and other things). *Methods in Ecology and Evolution* **3**: 217–223.

Rieseberg LH, Carney SE. 1998. Plant hybridization. *New Phytologist* **140**: 599–624. doi:10.1046/j.1469-8137.1998.00315.x.

Rieseberg LH, Wendel JF. 1993. Introgression and its consequences in plants. *Hybrid Zones and the Evolutionary Process* **70**: 109.

Rieseberg LH, Raymond O, Rosenthal DM, *et al.* 2003. Major ecological transitions in wild sunflowers facilitated by hybridization. *Science* **301**: 1211–1216. doi:10.1126/science.1086949.

Rifkin JL, Castillo AS, Liao IT, Rausher MD. 2019. Gene flow, divergent selection and resistance to introgression in two species of morning glories (*Ipomoea*). *Molecular Ecology* **28**: 1709–1729. doi:10.1111/mec.14945.

Saari S, Faeth SH. 2012. Hybridization of Neotyphodium endophytes enhances competitive ability of the host grass. *New Phytologist* **195**: 231–236. doi:10.1111/j.1469-8137.2012.04140.x.

Schemske DW. 2000. Understanding the Origin of Species 1. *Evolution* **54**: 1069–1073. doi:10.1554/0014-3820(2000)054[1069:utoos]2.3.co;2.

Schliep KP. 2011. phangorn: phylogenetic analysis in R. *Bioinformatics* **27**: 592–593. doi:10.1093/bioinformatics/btq706.

Shimodaira H, Hasegawa M. 1999. Multiple comparisons of log-likelihoods with applications to phylogenetic inference. *Molecular Biology and Evolution* **16**: 1114–1116. doi:10.1093/oxfordjournals.molbev.a026201.

Soltis DE, Visger CJ, Soltis PS. 2014. The polyploidy revolution then and now: Stebbins revisited. *American Journal of Botany* **101**: 1057–1078. doi:10.3732/ajb.1400178.

Soltis PS, Soltis DE. 2009. The role of hybridization in plant speciation. *Annual Review of Plant Biology* **60**: 561–588.

Stebbins GL. 1959. The role of hybridization in evolution. *Proceedings of the American Philosophical Society* **103**: 231–251.

Stelkens R, Seehausen O. 2009. Genetic distance between species predicts novel trait expression in their hybrids. *Evolution* **63**: 884–897. doi:10.1111/j.1558-5646.2008.00599.x.

Sujii PS, Cozzolino S, Pinheiro F. 2019. Hybridization and geographic distribution shapes the spatial genetic structure of two co-occurring orchid species. *Heredity* **123**: 458–469. doi:10.1038/s41437-019-0254-7.

Taylor SA, Larson EL. 2019. Insights from genomes into the evolutionary importance and prevalence of hybridization in nature. *Nature Ecology & Evolution* **3**: 170–177. doi:10.1038/s41559-018-0777-y.

Than C, Ruths D, Nakhleh L. 2008. PhyloNet: a software package for analyzing and reconstructing reticulate evolutionary relationships. *BMC Bioinformatics* **9**: 322. doi:10.1186/1471-2105-9-322.

Turner BL. 2006. Taxonomy and nomenclature of the *Erysimum asperum–E. capitatum* complex (Brassicaceae). *Phytologia* **88**: 279–287. doi:10.5962/bhl.part.10454.

UniProt Consortium. 2014. UniProt: a hub for protein information. *Nucleic Acids Research* **43**: D204–D212.

Wang D, Wang Z, Kang X, Zhang J. 2019. Genetic analysis of admixture and hybrid patterns of *Populus hopeiensis* and *P. tomentosa*. *Scientific Reports* **9**: 1–13.

Warwick SI, Francis A, Al-Shehba IA. 2006. Brassicaceae: species checklist and database on CD-Rom. *Plant Systematics and Evolution* **259**: 249–258.

Wen D, Yu Y, Zhu J, Nakhleh L. 2018. Inferring phylogenetic networks using PhyloNet. *Systematic Biology* **67**: 735–740.

Wu YC, Rasmussen MD, Bansal MS, Kellis M. 2014. Most parsimonious reconciliation in the presence of gene duplication, loss, and deep coalescence using labeled coalescent trees. *Genome Research* **24**: 475–486. doi:10.1101/gr.161968.113.

Yang Y, Smith SA. 2014. Orthology inference in nonmodel organisms using transcriptomes and low-coverage genomes: improving accuracy and matrix occupancy for phylogenomics. *Molecular Biology and Evolution* **31**: 3081–3092. doi:10.1093/molbev/msu245.

Yu Y, Nakhleh L. 2015. A maximum pseudo-likelihood approach for phylogenetic networks. *BMC Genomics* **16**: S10.

Zieliński P, Dudek K, Arntzen JW, *et al.* 2019. Differential introgression across newt hybrid zones: evidence from replicated transects. *Molecular Ecology* **28**: 4811–4824. doi:10.1111/mec.15251.

Züst T, Strickler SR, Powell AF, *et al.* 2020. Independent evolution of ancestral and novel defenses in a genus of toxic plants (*Erysimum*, Brassicaceae). *eLife* **9**: e51712.